All-optical wavelength conversion and signal regeneration of PAM-4 signal using a silicon waveguide

Yun Long,[1] Andong Wang,[1] Linjie Zhou,[2] and Jian Wang[1,*]

[1]*Wuhan National Laboratory for Optoelectronics, School of Optical and Electronic Information, Huazhong University of Science and Technology, Wuhan 430074, Hubei, China*

[2]*State Key Laboratory of Advanced Optical Communication Systems and Networks, Department of Electronic Engineering, Shanghai Jiao Tong University, Shanghai 200240, China*

[*]*jwang@hust.edu.cn*

Abstract: We experimentally demonstrate on-chip all-optical wavelength conversion of 10-Gbit/s (9.35-Gbit/s net rate) 4-level pulse amplitude modulation (PAM-4) signal by exploiting degenerate four-wave mixing (FWM) in a silicon waveguide. The measured optical signal-to-noise ratio (OSNR) penalty of wavelength conversion is ~1 dB at a bit-error rate (BER) of 2×10^{-3}. Moreover, the use of wavelength conversion for PAM-4 signal regeneration is also demonstrated in the experiment.

OCIS codes: (130.3120) Integrated optics devices; (190.4380) Nonlinear optics, four-wave mixing.

References and links

1. A. E. Willner, S. Khaleghi, M. R. Chitgarha, and O. F. Yilmaz, "All-optical signal processing," J. Lightwave Technol. **32**(4), 660–680 (2014).
2. M. Saruwatari, "All-optical signal processing for terabit/second optical transmission," IEEE J. Sel. Top. Quantum Electron. **6**(6), 1363–1374 (2000).
3. H. Dorren, M. Hill, Y. Liu, N. Calabretta, A. Srivatsa, F. Huijskens, H. De Waardt, and G. Khoe, "Optical packet switching and buffering by using all-optical signal processing methods," J. Lightwave Technol. **21**(1), 2–12 (2003).
4. X. Wu, "High-speed optical signal processing for terabit/second optical networks," in *Asia Communications and Photonics Conference* (Optical Society of America, 2012), paper AS2G.4.
5. S. J. B. Yoo, "Wavelength conversion technologies for WDM network applications," J. Lightwave Technol. **14**(6), 955–966 (1996).
6. J. M. H. Elmirghani and H. T. Mouftah, "All-optical wavelength conversion: technologies and applications in DWDM networks," IEEE Commun. Mag. **38**(3), 86–92 (2000).
7. T. Durhuus, B. Mikkelsen, C. Joergensen, S. L. Danielsen, and K. E. Stubkjaer, "All-optical wavelength conversion by semiconductor optical amplifiers," J. Lightwave Technol. **14**(6), 942–954 (1996).
8. S. Subramaniam, M. Azizoglu, and A. K. Soman, "All-optical networks with sparse wavelength conversion," IEEE Netw. Trans. **4**(4), 544–557 (1996).
9. S. You, C. Li, Q. Yang, M. Luo, Y. Qiu, X. Xiao, and S. Yu, "Seamless sub-band wavelength conversion of Tb/s-class CO-OFDM superchannels," IEEE Photonics Technol. Lett. **26**(8), 801–804 (2014).
10. C. Kachris and I. Tomkos, "A survey on optical interconnects for data centers," IEEE Comm. Surv. and Tutor. **14**(4), 1021–1036 (2012).
11. K. N. Georgakilas, A. Tzanakaki, M. Anastasopoulos, and J. M. Pedersen, "Converged optical network and data center virtual infrastructure planning," J. Opt. Commun. Netw. **4**(9), 681–691 (2012).
12. A. Wonfor, H. Wang, R. Penty, and I. White, "Large port count high-speed optical switch fabric for use within datacenters [Invited]," J. Opt. Commun. Netw. **3**(8), A32–A39 (2011).
13. B. Filion, W. C. Ng, A. T. Nguyen, L. A. Rusch, and S. Larochelle, "Wideband wavelength conversion of 16 Gbaud 16-QAM and 5 Gbaud 64-QAM signals in a semiconductor optical amplifier," Opt. Express **21**(17), 19825–19833 (2013).
14. R. Elschner, T. Richter, M. Nölle, J. Hilt, and C. Schubert, "Parametric amplification of 28-GBd NRZ-16QAM signals," in *Optical Fiber Communication Conference* (Optical Society of America, 2011), paper OThC2.
15. A. H. Gnauck, E. Myslivets, M. Dinu, B. P. P. Kuo, P. Winzer, R. Jopson, N. Alic, A. Konczykowska, F. Jorge, and J.-Y. Dupuy, "All-optical tunable wavelength shifting of a 128-Gbit/s 64-QAM signal," in *European Conference and Exhibition on Optical Communication* (Optical Society of America, 2012), paper Th.2.F.2.

#256115 Received 18 Dec 2015; revised 12 Mar 2016; accepted 12 Mar 2016; published 24 Mar 2016

16. G.-W. Lu, T. Sakamoto, and T. Kawanishi, "Wavelength conversion of optical 64QAM through FWM in HNLF and its performance optimization by constellation monitoring," Opt. Express **22**(1), 15–22 (2014).
17. W. Bogaerts, R. Baets, P. Dumon, V. Wiaux, S. Beckx, D. Taillaert, B. Luyssaert, J. Van Campenhout, P. Bienstman, and D. Van Thourhout, "Nanophotonic waveguides in silicon-on-insulator fabricated with CMOS technology," J. Lightwave Technol. **23**(1), 401–412 (2005).
18. M. A. Ettabib, K. Hammani, F. Parmigiani, L. Jones, A. Kapsalis, A. Bogris, D. Syvridis, M. Brun, P. Labeye, S. Nicoletti, and P. Petropoulos, "FWM-based wavelength conversion of 40 Gbaud PSK signals in a silicon germanium waveguide," Opt. Express **21**(14), 16683–16689 (2013).
19. H. Hu, H. Ji, M. Galili, M. Pu, C. Peucheret, H. C. H. Mulvad, K. Yvind, J. M. Hvam, P. Jeppesen, and L. K. Oxenløwe, "Ultra-high-speed wavelength conversion in a silicon photonic chip," Opt. Express **19**(21), 19886–19894 (2011).
20. R. Adams, M. Spasojevic, M. Chagnon, M. Malekiha, J. Li, D. V. Plant, and L. R. Chen, "Wavelength conversion of 28 GBaud 16-QAM signals based on four-wave mixing in a silicon nanowire," Opt. Express **22**(4), 4083–4090 (2014).
21. C. Li, C. Gui, X. Xiao, Q. Yang, S. Yu, and J. Wang, "On-chip all-optical wavelength conversion of multicarrier, multilevel modulation (OFDM m-QAM) signals using a silicon waveguide," Opt. Lett. **39**(15), 4583–4586 (2014).
22. Y. Long, J. Liu, X. Hu, A. Wang, L. Zhou, K. Zou, Y. Zhu, F. Zhang, and J. Wang, "All-optical multi-channel wavelength conversion of Nyquist 16 QAM signal using a silicon waveguide," Opt. Lett. **40**(23), 5475–5478 (2015).
23. R. Salem, M. A. Foster, A. C. Turner, D. F. Geraghty, M. Lipson, and A. L. Gaeta, "Signal regeneration using low-power four-wave mixing on silicon chip," Nat. Photonics **2**(1), 35–38 (2008).
24. Z. Kangping, Z. Xian, G. Yuliang, C. Wei, M. Jiangwei, Z. Li, A. P. T. Lau, and L. Chao, "140-Gb/s 20-km Transmission of PAM-4 Signal at 1.3 um for Short Reach Communications," IEEE Photonics Technol. Lett. **27**, 1757–1760 (2015).
25. S. Kota Pavan, J. Lavrencik, R. Shubochkin, Y. Sun, J. Kim, D. S. Vaidya, R. Lingle, T. Kise, and S. Ralph, "50Gbit/s PAM-4 MMF Transmission Using 1060nm VCSELs with Reach beyond 200m," in *Optical Fiber Communication Conference* (Optical Society of America, 2014), paper W1F.5.
26. X. Liu, X. Zhou, and C. Lu, "Four-wave mixing assisted stability enhancement: theory, experiment, and application," Opt. Lett. **30**(17), 2257–2259 (2005).
27. M. A. Foster, A. C. Turner, R. Salem, M. Lipson, and A. L. Gaeta, "Broad-band continuous-wave parametric wavelength conversion in silicon nanowaveguides," Opt. Express **15**(20), 12949–12958 (2007).
28. K. Yamada, H. Fukuda, T. Tsuchizawa, T. Watanabe, T. Shoji, and S. Itabashi, "All-optical efficient wavelength conversion using silicon photonic wire waveguide," IEEE Photonics Technol. Lett. **18**(9), 1046–1048 (2006).
29. W. Mathlouthi, H. Rong, and M. Paniccia, "Characterization of efficient wavelength conversion by four-wave mixing in sub-micron silicon waveguides," Opt. Express **16**(21), 16735–16745 (2008).

1. Introduction

All-optical signal processing is a promising technology for future optical transparent networks for its strong abilities to overcoming the electronics bottlenecks, supporting the ultra-fast optical signal processing without requiring costly optical-electrical-optical equipment [1–3]. High-speed all-optical signal processing functions, including wavelength conversion, signal regeneration, logic gate, format conversion, tunable optical delay, and so on, would play a crucial role in achieving flexible and low-latency management of network data traffic [4]. Specifically, wavelength conversion is of great importance for its ability to enhance the flexibility and optimize wavelength usage of future optical network [5–9]. Wavelength conversion is also considered to be a critical building block for optical routing applications in data centers [10–12]. All-optical wavelength conversions have been successfully demonstrated by several previous works based on optical nonlinearities in semiconductor optical amplifiers (SOAs) and highly nonlinear fibers (HNLFs). Wavelength conversion of 16-Gbaud 16-ary quadrature amplitude modulation (16-QAM) and 5-Gbaud 64-QAM was demonstrated based on four-wave mixing (FWM) in an SOA using a dual-pump configuration [13]. Wavelength conversion of 16-QAM and 64-QAM signal based on HNLFs was also realized [14–16]. Compared to SOAs and HNLFs, silicon-on-insulator (SOI) waveguides feature low cost, ultra-compact footprint and complementary metal-oxide-semiconductor (CMOS) compatibility [17]. Also, the tight light confinement of silicon waveguides will greatly enhance the nonlinear effects. FWM-based wavelength conversions of 80-Gbit/s differential quadrature phase shift key (DQPSK) signals [18], 640-Gbit/s return-

#256115 Received 18 Dec 2015; revised 12 Mar 2016; accepted 12 Mar 2016; published 24 Mar 2016

to-zero differential phase shift keying (RZ-DPSK) signals [19], and 112-Gbit/s 16-QAM signals [20] have been demonstrated in silicon waveguides. By combining orthogonal frequency division multiplexing (OFDM) with advanced multilevel signals, on-chip all-optical wavelength conversion of multicarrier multilevel modulation signals has been demonstrated [21]. Moreover, on-chip multi-channel wavelength conversion of Nyquist 16-QAM signal has been realized for multi-channel applications [22]. In addition, the use of FWM in silicon waveguides for signal regeneration of on-off keying (OOK) signal has also been demonstrated [23].

Due to the simple setup configuration and relatively lower requirement of modulation depth and linearity than m-QAM, pulse amplitude modulation (PAM) is suitable for low cost and high capacity transmissions [24, 25] such as metro networks. High speed transmission of PAM-4 signal has been demonstrated in many previous works, which has shown superior advantages of PAM-4 in short reach communication. Using all-optical signal processing technology may further enhance the reconfigurability and flexibility of PAM-4 optical communication systems. To the best of our knowledge, there has been limited research in all-optical signal processing of PAM-4, especially on-chip PAM-4 signal processing using silicon waveguides.

In this paper, we comprehensively characterize on-chip wavelength conversion of PAM-4 signal by exploiting FWM in a silicon waveguide. Two cases, i.e. traditional wavelength conversion and signal regeneration are discussed in detail. Low-penalty traditional wavelength conversion and efficient signal regeneration are demonstrated in the experiment using a 10-Gbit/s (9.35-Gbit/s net rate) PAM-4 signal.

2. Concept and operation principle

Figure 1 illustrates the concept and principle of all-optical wavelength conversion and signal regeneration of PAM-4 signal in a silicon waveguide. One continuous-wave (CW) pump and a data carrying signal (S) are fed into the silicon waveguide. When propagating along the silicon waveguide, pump photons are annihilated to create signal photons and newly converted idler 1 photons by the degenerate FWM process. Meanwhile, signal photons are also consumed to generate pump photons and newly converted idler 2 photons by the degenerate FWM process. At the output of the silicon waveguide, the data information carried by the input signal is converted to the idlers. Two converted idlers (idler 1, idler 2) are generated by the degenerate FWM processes. Under non-depletion approximation, the powers of the two idlers can be expressed as $P_{i1} \propto \gamma^2 L_{eff}^2 P_s P_p^2$ (idler1) and $P_{i2} \propto \gamma^2 L_{eff}^2 P_p P_s^2$ (idler2), respectively, where γ is the nonlinear coefficient of the waveguide, L_{eff} is the effective interaction length of FWM, P_s and P_p are the power of the signal and pump light [26]. There are two cases with different input signals, as shown in Figs. 1(b) and 1(c). In Case 1 of traditional wavelength conversion, the input signal is a standard PAM-4 signal with uniform power intervals among four power levels. Thus idler 1, having linear relationship of optical power with input signal, keeps uniform power intervals. In contrast, the converted idler 2 becomes distorted with nonuniform power intervals. As a result, in Case 1 (from input signal to converted idler 1) the information carried by the input PAM-4 signal S is converted to idler 1 with favorable conversion performance. In Case 2 of signal regeneration, the input distorted PAM-4 signal has nonuniform power intervals among four power levels. If a uniform PAM-4 signal is degraded to a nonuniform signal like the input distorted signal shown in Fig. 1(c), the idler 2, having square power relationship with the input signal, is regenerated with uniform power intervals. For comparison, the converted idler 1 still has nonuniform power intervals. As a consequence, in Case 2 (from input signal to converted idler 2) the degenerate FWM process can be also used for signal regeneration of distorted PAM-4 signal.

#256115 Received 18 Dec 2015; revised 12 Mar 2016; accepted 12 Mar 2016; published 24 Mar 2016

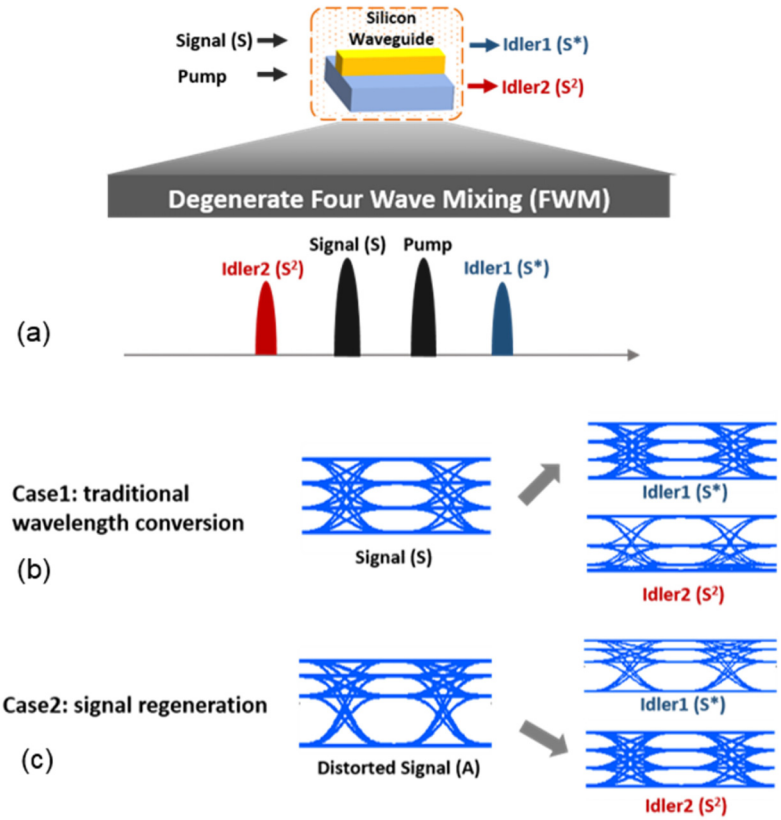

Fig. 1. Concept and principle of all-optical wavelength conversion and signal regeneration of PAM-4 signal in a silicon waveguide. Case 1: traditional wavelength conversion; Case 2: signal regeneration.

The normalized power levels of PAM-4 signal can be written by a, b, c, and 1, where $0<a<b<c<1$. For an ideal PAM-4 signal with uniform power intervals, a, b, and c satisfy $(b-a) = (c-b) = (1-c)$. Since the power of the lowest power level a is much smaller than the other power levels in our experiment, we assume $a = 0$. For Case 1 with standard PAM-4 signal input with uniform power intervals, the ideal normalized power levels are 0, 1/3, 2/3, and 1. After wavelength conversion, idler 1 will remain uniform power intervals while the four normalized power levels of idler 2 become 0, 1/9, 4/9, and 1. In Case 2, the input distorted PAM-4 signal has nonuniform power intervals among four power levels. To realize perfect signal regeneration,according to the quadratic dependence of the power of idler 2 on the input signal, the power level of the input distorted PAM-4 signal should be 0, $\sqrt{1/3}$, $\sqrt{2/3}$, and 1.

3. Experimental results

Fig. 2. Photomicrograph of the fabricated silicon waveguide.

#256115 Received 18 Dec 2015; revised 12 Mar 2016; accepted 12 Mar 2016; published 24 Mar 2016

The photomicrograph of the fabricated silicon waveguide is shown in Fig. 2. The silicon waveguide employed in the experiment is a 6-mm-long SOI strip waveguide with a cross section of 500 nm width and 220 nm thick. The waveguide is coated with a SiO_2 layer. The transmission loss of the waveguide is estimated to be 3~4 dB/cm. Vertical grating couplers are used to couple light in/out of the silicon waveguide and ensure operation with TE-polarized light. The measured transmission of the grating couplers (contain both input and output couplers) is shown in Fig. 3. The propagation loss has been subtracted. It can be seen from Fig. 3 that the grating coupling loss is about 6~7 dB per facet around 1550 nm.

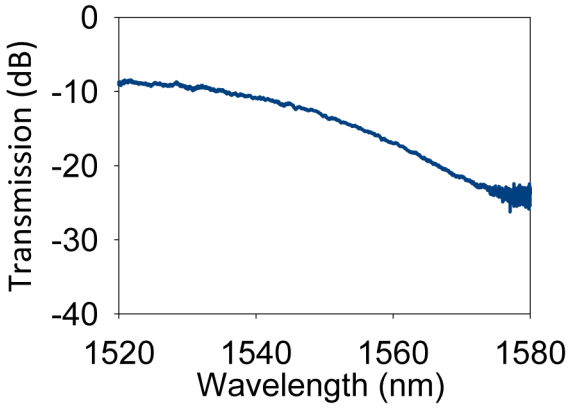

Fig. 3. Measured transmission of the grating couplers.

The expected dispersion of the waveguide is shown in Figs. 4-10 dB conversion bandwidth is expected to be more than 60 nm with 1550 nm pump according to our calculation using a similar method as ref [27].

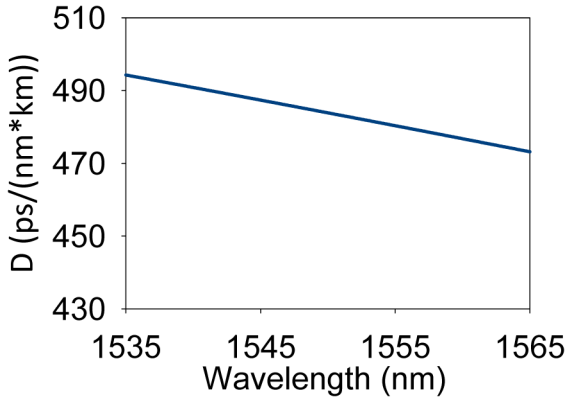

Fig. 4. Expected dispersion of the silicon waveguide.

The experimental setup for silicon waveguide based PAM-4 wavelength conversion and signal regeneration is shown in Fig. 5. The wavelengths of input PAM-4 signal and CW pump fed into silicon waveguide are 1550.13 and 1553.35 nm, respectively. At the transmitter, CW output from an external cavity laser (ECL1) serves as the signal light for the degenerate FWM process. The signal light is then modulated with PAM-4 at 5 Gbaud by an optical intensity modulator. An arbitrary waveform generator (AWG) is used to produce the electrical signal. The modulated signal is then amplified by an erbium-doped optical fiber amplifier (EDFA1). Afterwards, the PAM-4 signal is combined with another CW light from ECL2 serving as the pump light through a coupler. Polarization controllers (PC2 and PC3)

#256115 Received 18 Dec 2015; revised 12 Mar 2016; accepted 12 Mar 2016; published 24 Mar 2016

are used to adjust the polarization states of the input signal and pump light to achieve optimized conversion efficiency of degenerate FWM process. After wavelength conversion or signal regeneration, the desired idler is selected using two stage optical filtering (TF3, TF4). First, the desired idler is selected using TF3. Since the power level of the idler is relatively low, the selected idler is amplified by EDFA3. Second, in order to suppress the amplified spontaneous emission (ASE) noise originated from the EDFA3, another TF4 is employed. At the receiver, the optical signal is first detected by a standard direct detection photodetector and then sent to a real-time digital oscilloscope (Keysight DSA-Z 204A) operating at 80 GS/s with a bandwidth of 20 GHz. Then the sampled signal is processed offline using MATLAB. The sampled signal is first normalized and re-sampled to 2 sample-per-symbol. Then, an adaptive linear equalization filter is utilized for channel equalization. After symbol decision with three threshold levels, the bit-error rate (BER) was calculated by error counting. The received optical signal-to-noise ratio (OSNR) is monitored before the photodetector as shown in Fig. 5.

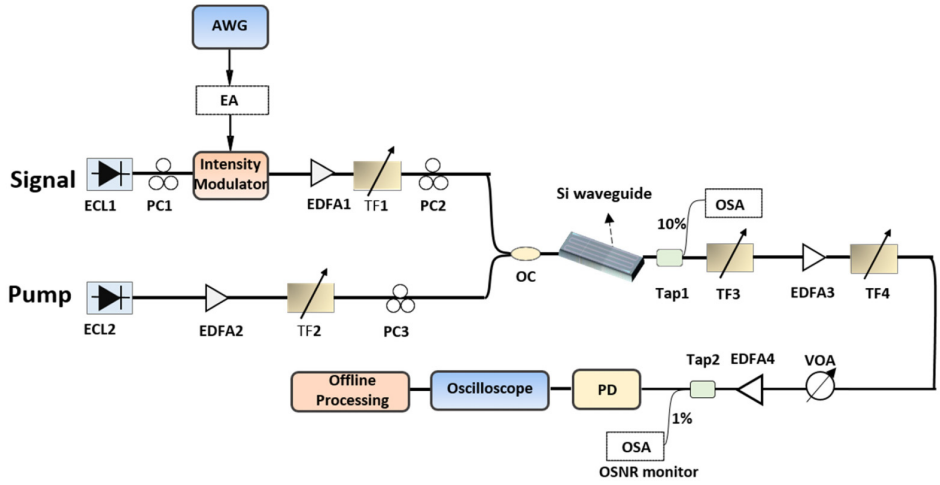

Fig. 5. Experimental setup for silicon waveguide based PAM-4 wavelength conversion and signal regeneration in a silicon waveguide. ECL: external cavity laser; AWG: arbitrary waveform generator; EDFA: erbium-doped fiber amplifier; PC: polarization controller; OC: optical coupler; TF: tunable filter; OSA: optical spectrum analyzer; VOA: variable optical attenuator; PD: photodetector.

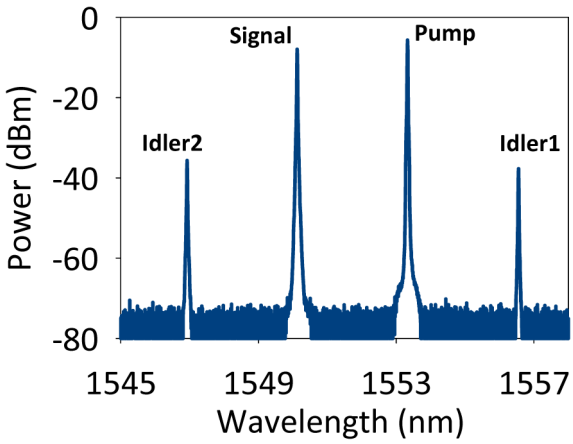

Fig. 6. Measured spectrum of degenerate FWM process in the silicon waveguide.

#256115 Received 18 Dec 2015; revised 12 Mar 2016; accepted 12 Mar 2016; published 24 Mar 2016

The measured spectrum of degenerate FWM process in the silicon waveguide is shown in Fig. 6, which is monitored at Tap1 coupler after the silicon chip. The powers of the input pump and signal are about 15.5 and 13.5 dBm, respectively. The light powers here are the collected power in the silicon waveguide taking into account the coupling loss of the input grating coupler. When the pump and signal light are coupled into the waveguide, two converted idlers (idler 1: 1556.55 nm, idler 2: 1546.93 nm) are generated, which can be clearly seen in Fig. 6. The angular frequencies of the generated idlers are $\omega_{idler1} = 2\omega_{pump} - \omega_{signal}$ and $\omega_{idler2} = 2\omega_{signal} - \omega_{pump}$, respectively. The optical power of idler 1 is slightly smaller than idler 2 in Fig. 6, which is due to the coupling loss difference of grating coupler between the wavelengths of idler 1 and idler 2 as shown in Fig. 3. We define the conversion efficiency as the power ratio of converted idler to signal. The conversion efficiencies of idler 1 and idler 2 are –28.49 dB and –29.27 dB, respectively. The wavelength dependent loss of the output grating coupler has been taken into consideration when calculating the conversion efficiency.

To evaluate the conversion bandwidth of the waveguide experimentally, we measure the conversion efficiency as a function of the signal wavelength when the wavelength of pump light is 1553.35 nm. The powers of the input pump and signal are set to be 15 and 12.4 dBm, resepectively. Figure 7 shows the measured conversion efficiencies of idler 1 and idler 2.

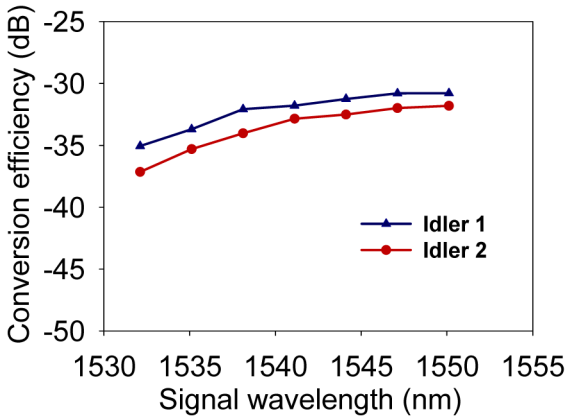

Fig. 7. Measured conversion efficiencies as a function of signal light wavelength when the pump wavelength is fixed at 1553.35 nm.

As previously mentioned, the relations between the idlers power and signal power can be written as $P_{i1} \propto P_s$ and $P_{i2} \propto P_s^2$. We further experimentally examine this theoretical prediction. Figure 8 shows the measured idlers power as functions of signal power. The wavelengths of input signal and pump fed into silicon waveguide are 1550.13 and 1553.35 nm, respectively. The linear dependence of idler 1 power on the signal power and the quadratic dependence of idler 2 power on the signal power are clearly shown in Fig. 8. Since the input power level is relatively low in the experiment, no significant saturation of the idler power versus signal power is observed in the experiment.

#256115 Received 18 Dec 2015; revised 12 Mar 2016; accepted 12 Mar 2016; published 24 Mar 2016

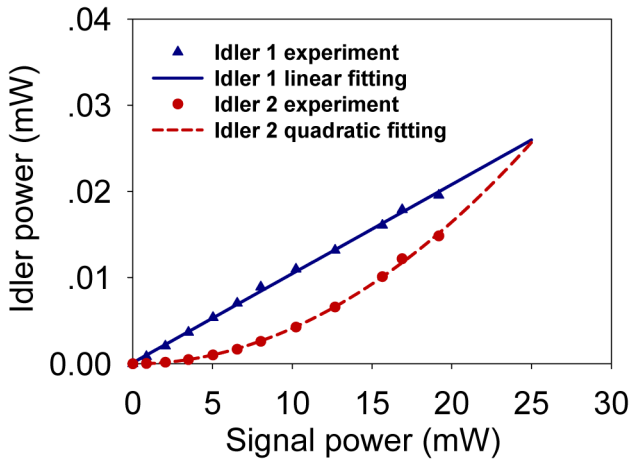

Fig. 8. Measured idler powers as a function of signal power.

We further evaluate the system performance of the proposed scheme of all-optical wavelength conversion and signal regeneration of PAM-4 signal. The powers of the input pump and signal are about 15.5 and 13.5 dBm for all the configurations below. Figure 9 shows the measured eye diagrams and BER performance of back to back (B-to-B), idler 1, and idler 2 in Case 1 and Case 2, respectively. In Case 1, a standard PAM-4 signal with uniform power intervals is used as the input signal. The normalized power levels of the input signal are 0, 1/3, 2/3, and 1. Idler 1 is also uniform, while idler 2 is degraded. The corresponding BER performance as a function of received optical OSNR is also shown in Fig. 9(b). The measured OSNR penalty of wavelength conversion from input PAM-4 signal to converted idler 1 is around 1 dB at a BER of 2×10^{-3} (enhanced forward error correction (EFEC) threshold), showing favorable conversion performance for silicon waveguide based traditional wavelength conversion applications. Considering the 7% overhead with the threshold of EFEC, the net rate of the used 10-Gbit/s PAM-4 signal is 9.35 Gbit/s. In Case 2, the power levels of the input distorted PAM-4 signal are set to be 0, $\sqrt{1/3}$, $\sqrt{2/3}$, and 1. Since the distorted input signal is nonuniform, it could not be analyzed by the receiver. After degenerate FWM process, the power level interval of idler 1 is nonuniform, while the spacing between consecutive power levels of the idler 2 is a constant, which can be seen from Fig. 9(c). As clearly shown in Fig. 9(d), the BER performance of converted idler 2 is greatly improved compared to the input signal, which indicates the successful implemenation of degenerate FWM based wavelength conversion for signal regeneration of distorted PAM-4 signal.

#256115 Received 18 Dec 2015; revised 12 Mar 2016; accepted 12 Mar 2016; published 24 Mar 2016

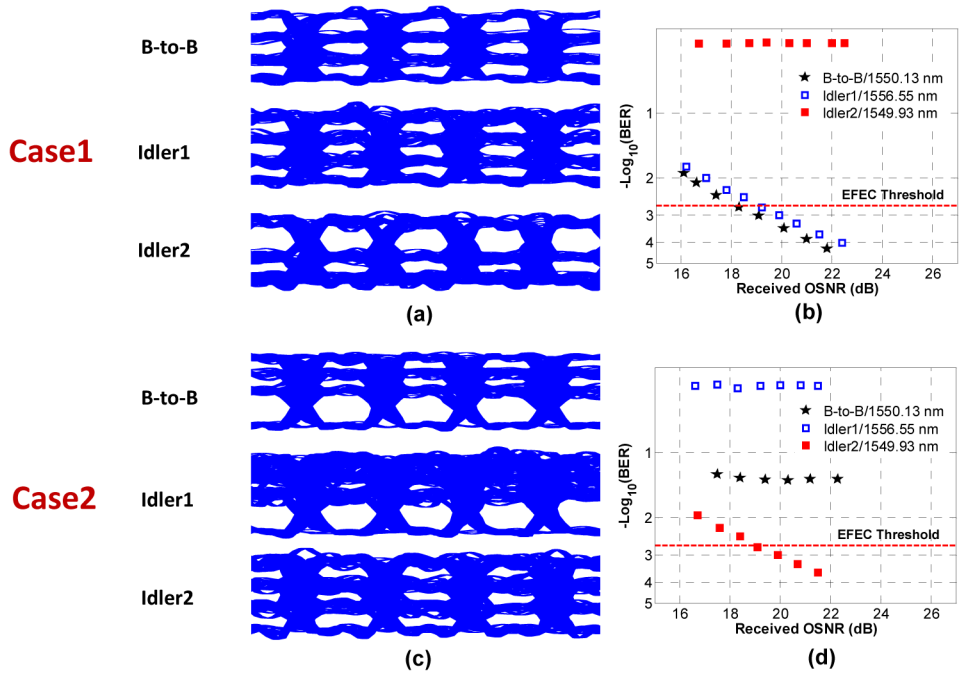

Fig. 9. Measured (a)(c) eye diagrams and (b)(d) BER performance of B-to-B signal, converted idler 1 and idler 2 in (a)(b) Case 1 and (c)(d) Case 2, respectively.

We further evaluate the intermediate state between Case 1 and Case 2. The normalized power levels of the input distorted signal are 0, 0.46, 0.73, and 1. The expected normalized power levels of idler 2 are 0, 0.21, 0.53, and 1. The measured eye diagrams and BER performance are shown in Fig. 10. It can be seen from Fig. 10 that the BER performance of B-to-B signal, converted idler 1 and idler 2 of the intermediate state are all between Case 1 and Case 2. The BER performance of B-to-B and idler 1 are better than Case 2 while worse than Case 1. The BER performance of idler 2 is better than Case 1 while worse than Case 2.

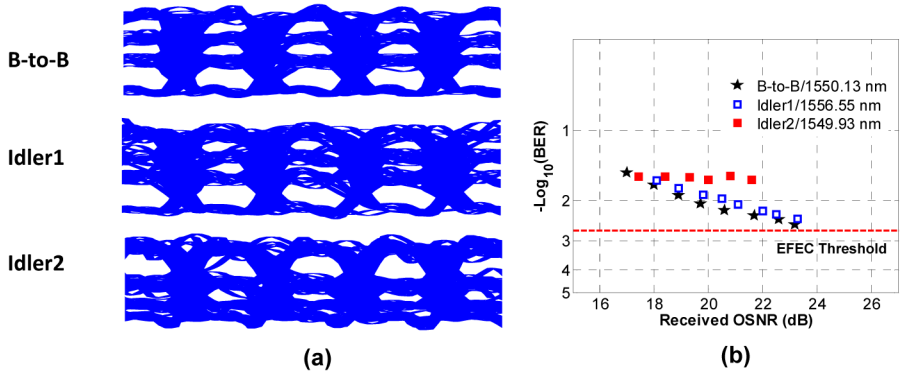

Fig. 10. Measured (a) eyes diagrams and (b) BER performance of B-to-B signal, converted idler 1 and idler 2 in the intermediate state between Case 1 and Case 2.

4. Discussion

As shown in Fig. 8, idler 1 power has linear dependence on the signal power, and idler 2 power has quadratic dependence on the signal power. Remarkably, with further increase of the signal power, saturation of the idler powers (idler 1, idler 2) is expected [23, 28, 29].

#256115 Received 18 Dec 2015; revised 12 Mar 2016; accepted 12 Mar 2016; published 24 Mar 2016

Thus, when considering the saturation of the idler under high power signal, idler 1 has a linear relation to the signal power in low power region and is saturated in high power region, while idler 2 has a quadratic relation to the signal power in low power region and is also saturated in high power region. Beyond using the aforementioned linear/quadratic wavelength conversion, one might also use wavelength conversion in saturation region to realize more complicated signal regeneration operations. In general, there are three cases which could be used for signal regeneration: 1) quadratic wavelength conversion; 2) quadratic wavelength conversion with saturation; 3) traditional linear wavelength conversion with saturation. Moreover, by cascading two wavelength converters, more kinds of distortions might be compensated. As a consequence, depending on different kinds of distorted input signals, which might originate from the nonlinear response of modulator or fiber transmission link, one might choose different corresponding working conditions to enable adjustable all-optical signal regeneration. Additionally, by changing the CW pump to a clock pump, the proposed scheme might also be used for signal retiming to further improve the regeneration performance [23].

5. Conclusion

In summary, we comprehensively characterize on-chip wavelength conversion of PAM-4 signal by using degenerate FWM in a silicon waveguide. Two cases, i.e. traditional wavelength conversion and signal regeneration are discussed in detail. Low penalty (~1 dB) traditional wavelength conversion and favorable signal regeneration are demonstrated in the experiment. With future improvement, more and more on-chip optical signal processing applications of PAM signal might be facilitated by exploiting optical nonlinearities in silicon waveguides.

Acknowledgments

This work was supported by the National Natural Science Foundation of China (NSFC) under grants 61222502 and 11574001, the Program for New Century Excellent Talents in University (NCET-11-0182), the Wuhan Science and Technology Plan Project under grant 2014070404010201, and the seed project of Wuhan National Laboratory for Optoelectronics (WNLO). The authors thank the Center of Micro-Fabrication and Characterization (CMFC) of WNLO and the facility support of the Center for Nanoscale Characterization and Devices of WNLO.

#256115 Received 18 Dec 2015; revised 12 Mar 2016; accepted 12 Mar 2016; published 24 Mar 2016